NACA

RESEARCH MEMORANDUM

for the

Bureau of Aeronautics, Department of the Navy

A TRANSONIC WIND-TUNNEL INVESTIGATION OF A SEAPLANE CONFIGURATION HAVING A 40° SWEPTBACK WING

TED NO. NACA DE 387

By Gerald Hieser, Louis Kudlacik, and W. H. Gray

Langley Aeronautical Laboratory
Langley Field, Va.

NATIONAL ADVISORY COMMITTEE
FOR AERONAUTICS

WASHINGTON

APR 1955

NATIONAL ADVISORY COMMITTEE FOR AERONAUTICS

RESEARCH MEMORANDUM

for the

Bureau of Aeronautics, Department of the Navy

A TRANSONIC WIND-TUNNEL INVESTIGATION OF A SEAPLANE CONFIGURATION HAVING A 40° SWEPTBACK WING

TED NO. NACA DE 387

By Gerald Hieser, Louis Kudlacik, and W. H. Gray

SUMMARY

During the course of an aerodynamic loads investigation of a model of the Martin XP6M-1 flying boat in the Langley 16-foot transonic tunnel, longitudinal-aerodynamic-performance information was obtained. Data were obtained at speeds up to and exceeding those anticipated for the seaplane in level flight and included the Mach number range from 0.84 to 1.09. The angle of attack was varied from -2° to 6° and the average Reynolds number, based on wing mean aerodynamic chord, was about 3.7×10^6.

This seaplane, although not designed to maintain level flight at Mach numbers beyond the force break, was found to have a transonic drag-rise coefficient of 0.0728, with an accompanying drag-rise Mach number of about 0.85. A large portion of the drag rise and the relatively low value of drag-rise Mach number result from the axial coincidence of the maximum areas of the principal airplane components.

INTRODUCTION

As the size and load-carrying capabilities of aircraft have increased along with increases in engine thrust, larger and larger landing fields have been required. The seaplane affords more flexibility in choice of landing areas and length of run for landing and take-off. However, these advantages are somewhat offset by several difficult problems. There is first the hydrodynamic problem of water impact loads and spray effects in light and heavy seas. Secondly, there is the aerodynamic problem of combining seaworthiness with good aerodynamic efficiency.

The Martin XP6M-1 flying boat represents a recent approach to a compromise between the seaworthiness and high-speed potentiality requirements. This seaplane was designed to fly at high subsonic speeds and to operate in and out of relatively heavy seas. The latter requirement, which leads to spray problems, dictated a high engine-nacelle placement. This placement of the nacelles, however, contributes to a large concentration of cross-sectional area resulting in a poor area distribution of the overall configuration.

One structural requirement of the airplane is that it must dive and recover at Mach numbers exceeding those expected in level flight. As a result of this requirement, the Bureau of Aeronautics, Department of the Navy, requested an aerodynamic loads investigation of the model in the Langley 16-foot transonic tunnel at Mach numbers up to the limit of the facility. During this investigation, the model's longitudinal aerodynamic characteristics were determined at Mach numbers from 0.84 to 1.09 and angles of attack from -2° to 6° and are reported herein. The results of an investigation of the hydrodynamic characteristics of a model of the XP6M-1 are given in reference 1.

COEFFICIENTS AND SYMBOLS

All coefficients and symbols used in the present paper are defined in the following list. All moments are referred to the quarter-chord point of the mean aerodynamic chord, both axially and vertically.

C_L lift coefficient, Lift/qS

C_D drag coefficient, Drag/qS

C_{D_i} nacelle internal-drag coefficient, $\frac{\text{Internal drag}}{qS}$

C_m pitching-moment coefficient, $\frac{\text{Pitching moment}}{qS\bar{c}}$

q dynamic pressure, $\frac{1}{2}\rho V^2$, lb/sq ft

S wing area, 3.852 sq ft

$\bar{c}$ wing mean aerodynamic chord, $\frac{2}{S}\int_0^{b/2} c^2 dy$, ft

c local wing chord, ft

A	model cross-sectional area, sq ft
b	wing span, ft
V	free-stream velocity, ft/sec
M	Mach number
i_t	tail incidence, deg; angle between stabilizer chord and wing root chord
X	longitudinal distance from body nose, ft
l	length of body, ft
α	angle of attack, deg; angle between free stream and wing root chord
ρ	air density, slugs/cu ft
$dC_L/d\alpha$	lift-curve slope
dC_m/dC_L	longitudinal-stability parameter

MODELS AND APPARATUS

Model Characteristics

A three-view drawing of the seaplane model of the Martin XP6M-1 is shown in figure 1, and a photograph of the model installed on its sting support system in the Langley 16-foot transonic tunnel is shown in figure 2.

The wing has an aspect ratio of 5.26 and a taper ratio of 0.333 with a sweep of the quarter-chord line of 40°. The airfoil section at the root is NACA 63A311 streamwise and at the tip is NACA 63A308 streamwise. The incidence of the root is 3.0° relative to the waterline and the tip is washed out 5° relative to the root, thus giving the tip an angle of -2.0° relative to the waterline. The leading edge of the nacelles is swept back spanwise along a constant $2\frac{1}{2}$ percent chord of the wing.

The physical arrangement of the model has been altered slightly at the afterbody from that of the actual airplane in order to permit clearance for the sting and model deflections. The modifications are outlined in figure 1 and are also apparent in the photograph of figure 2.

The cross-sectional-area development of the airplane obtained by cutting planes normal to the model axis is shown in figure 3. This figure has not been adjusted for after-fuselage modifications of the model.

Instrumentation

The model forces and moments were measured by a six-component strain-gage balance. The model angle of attack was determined from the static angle of attack corrected for deflections under load. These deflections had been established during static calibration of the model and balance.

Mass-flow ratios and internal drag were evaluated by rakes installed in the nacelle exits. The flow quantities were evaluated in tests other than those used to determine the aerodynamic characteristics. The model base pressures were measured by orifices located just inside the model base on the supporting sting.

Tunnel and Supporting System

The investigation was conducted in the Langley 16-foot transonic tunnel which has an octagonal slotted test section permitting continuous variation in speed through transonic to low supersonic speeds. The sting support system is designed to maintain the model close to the tunnel center line at all angles of attack.

TESTS AND CORRECTIONS

Because of the low design load factors required of this airplane and of the balance limiting loads, the angle-of-attack range was generally between the limits of -3° and 6°. At the highest Mach number tested (1.09), tunnel power limitations further restricted the angle-of-attack range. The angle of attack, referred to the wing root chord, is estimated to be correct within $\pm 0.1^{\circ}$. In order to obtain the published values, adjustments have been made for model support and balance deflections under load.

The Mach number recorded is believed to be accurate within ± 0.005. The data at low supersonic Mach numbers are affected somewhat by boundary-reflected disturbances impinging on the model. It has been estimated that the present model in the Langley 16-foot transonic tunnel should be free of all such disturbances at Mach numbers above about 1.09.

No corrections have been applied for sting interference, but the error so introduced is believed to be small. An adjustment has been made

to the force data to the condition of free-stream static pressure at the model base. The internal-flow drag of the nacelles has been subtracted from the drag measurements.

The variation of Reynolds number with Mach number for this investigation is presented in figure 4. The values are based on the mean aerodynamic chord and averaged about 3.7×10^6.

RESULTS AND DISCUSSION

Internal Drag

The internal drag was essentially invariant with angle of attack but was affected by Mach number (fig. 5). Internal-drag coefficient (based on wing area) increased 43 percent between Mach numbers of 0.84 and 1.00. The average mass-flow ratio based on inlet area was 0.75. The internal drag was evaluated to a Mach number of 1.06, but an extrapolation was made (dotted line in fig. 5) to a Mach number of 1.09 in order that the drag coefficients at this Mach number could be adjusted for internal drag.

Aerodynamic Characteristics

Basic data.- The basic data are shown in figures 6 to 9. The characteristics of the airplane without the horizontal tail are presented in figure 6, and those for the complete airplane with the horizontal tail set at angles of -0.82° and -3.02° are presented in figures 7 and 8, respectively. Figure 9 presents the characteristics of the model without the engine nacelles.

The angle-of-attack range of the investigation was not sufficient to define any gross nonlinearities in either the lift or pitching-moment coefficients. The lift-coefficient limit of the investigation was about 0.5.

Lift-curve slope.- The lift-curve slope, measured at zero lift, averaged about 0.086 throughout the Mach number range as indicated in figure 10. The theoretical value of lift-curve slope for a wing of this aspect ratio and taper ratio at a Mach number of 0.84 is 0.075. Apparently, there is an appreciable increase in effective aspect ratio because of the end-plate effect of the tip floats. In addition, the theory would not be expected to predict the lift-curve slope accurately for this specific configuration.

[redacted]

Static-longitudinal-stability parameter.- The variation of the static-longitudinal-stability parameter dC_m/dC_L at zero lift for the Mach number range from 0.84 to 1.03 indicates a rearward aerodynamic-center movement of 21 percent for the tail-off configuration (fig. 11). The change in magnitude of dC_m/dC_L for both tail-on and tail-off configurations indicates an abrupt forward aerodynamic-center shift of about 8 percent which was measured at Mach numbers of 0.95 and 0.975 for the former configuration and at a Mach number of 0.975 only for the latter configuration. An explanation for the reduction in stability in this narrow Mach number band could not be found from a study of loading changes shown by unpublished wing and nacelle pressure data. It is believed, however, that the abrupt reduction in stability arises from a rapid variation in stream direction behind the nacelles over the rear portion of the body as the angle of attack is varied. This change in stream direction is apparently caused by strong vertically asymmetric shocks in the vicinity of the nacelle exit at Mach numbers of 0.95 and 0.975 and is confined to a small lift range near zero. Some verification of this reasoning may be obtained from inspection of the dC_m/dC_L values for the model with the nacelles removed. The latter curve (fig. 11), although based on fewer test points than for the nacelle installed, appears, nevertheless, to be devoid of abrupt slope changes and, therefore, justifies the reasoning.

Drag.- The zero-lift drag coefficient and drag coefficient at a lift coefficient of 0.3 are presented in figure 12. The configurations chosen for this figure all had a tail incidence of -3.02°. For this tail setting, the model trimmed at about an average lift coefficient of -0.05.

The limit test Mach number of 1.09 was sufficiently high to permit wall-reflected disturbances to clear the base of the model. The probable trend of the zero-lift drag curve for the complete model between the Mach numbers of 1.00 and 1.09 has also been indicated on figure 12. The measured drag in this range of Mach number is affected by wall-reflected disturbances which impinge on the forepart of the body in the lower portion of this range, thus increasing drag to an artificially high value, and on the body aft of the maximum cross-sectional area in the higher portion of the range, thus reducing drag.

This seaplane, although not designed to maintain level flight at Mach numbers beyond the force break, was found to have a transonic drag-rise coefficient of 0.0728. A large portion of this drag rise may be attributed to the concentration of cross-sectional area of the principal airplane components as shown on the area plot of figure 3. A further and perhaps more significant result of this area distribution is the low force-break Mach number of about 0.85 (the Mach number at which $dC_D/dM \approx 0.1$). For example, removing the nacelles improves the area distribution somewhat (fig. 3) and increases the force-break Mach number by about 0.020. (See fig. 12.)

[redacted]

The rather intense shocks generated by the large cross-sectional area are shown in the sample shadowgraphs of figure 13. The intensity of the shocks in the vicinity of the nacelles is probably an indication of concentration of these shocks in a spanwise as well as chordwise direction. Removing the nacelles had a large effect in reducing the apparent intensity of the shocks but had very little effect on their position, as would be expected from an inspection of figure 3.

CONCLUSIONS

Longitudinal-performance information obtained during an aerodynamic loads investigation of a model of the Martin XP6M-1 flying boat at transonic speeds leads to the following conclusions:

1. The model has a transonic drag-rise coefficient of 0.0728 and a drag-rise Mach number of about 0.85. A large portion of the drag rise, as well as the low value of drag-rise Mach number, results from the axial coincidence of the maximum cross-sectional areas of the principal airplane components. No other predominant characteristics were found in the aerodynamic data.

2. The aerodynamic center shifts rearward 21 percent of the mean aerodynamic chord with increase in Mach number from 0.84 to 1.03. The gradual progression of the aerodynamic center is interrupted at a Mach number of about 0.975 by an abrupt forward shift of 8 percent. It is believed that the strong shocks in the vicinity of the nacelle exit caused a rapid adjustment in stream direction behind the nacelles and a resulting reduction in stability.

Langley Aeronautical Laboratory,
National Advisory Committee for Aeronautics,
Langley Field, Va., March 18, 1955.

Gerald Hieser
Aeronautical Research Scientist

Louis Kudlacik
Mechanical Engineer

W. H. Gray
Aeronautical Research Scientist

Approved: Eugene C. Draley
Eugene C. Draley
Chief of Full-Scale Research Division

mld [redacted]

REFERENCE

1. Carter, Arthur W., and Blanchard, Ulysse J.: Tank Investigation of the Hydrodynamic Characteristics of a 1/13.33-Scale Jet-Powered Dynamic Model of the Martin XP6M-1 Flying Boat - TED No. NACA DE 385. NACA RM SL55D06, Bur. Aero., 1955.

[redacted]

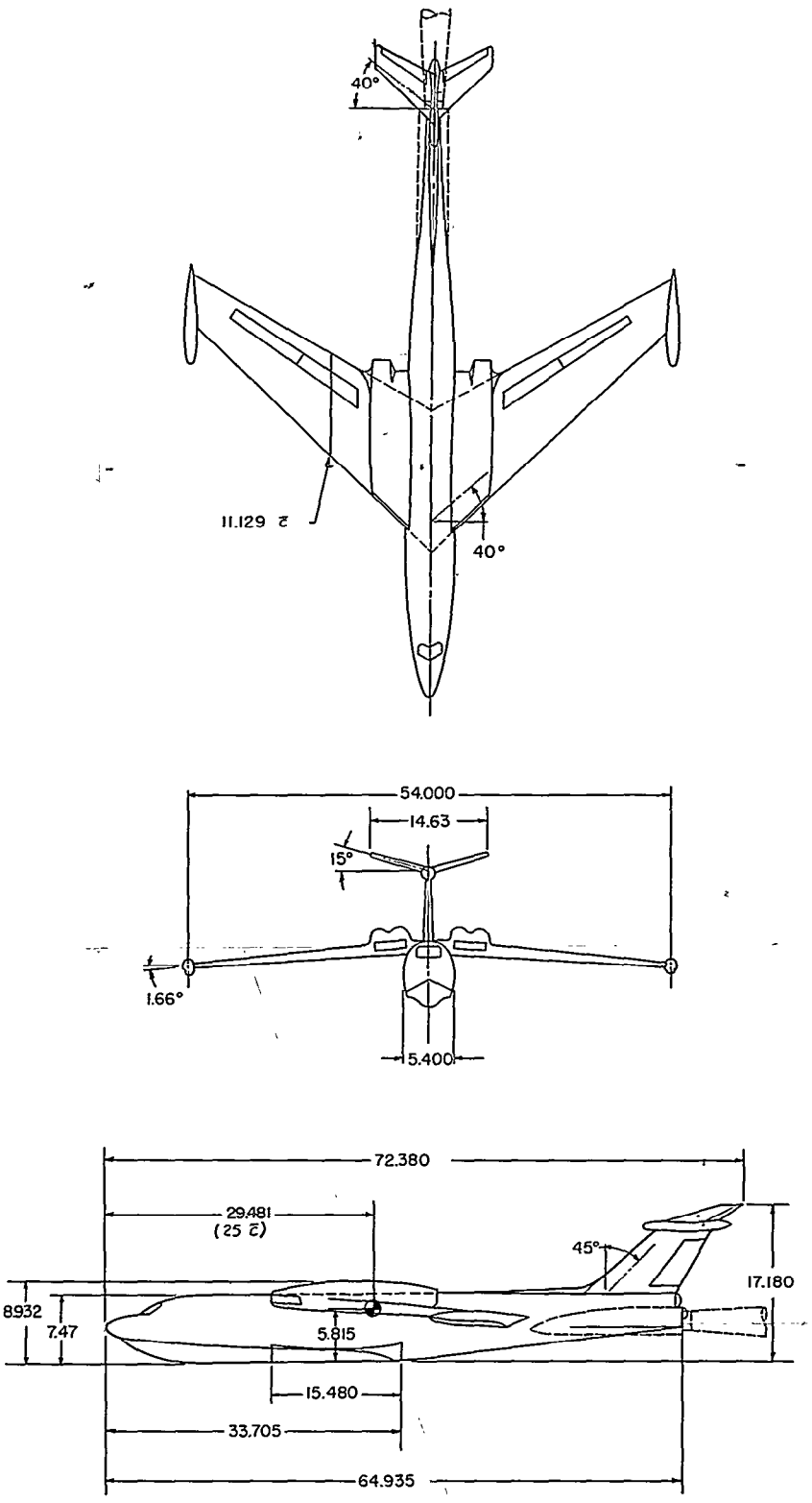

Figure 1.- Sketch of the 0.045-scale wind-tunnel model. All dimensions are in inches.

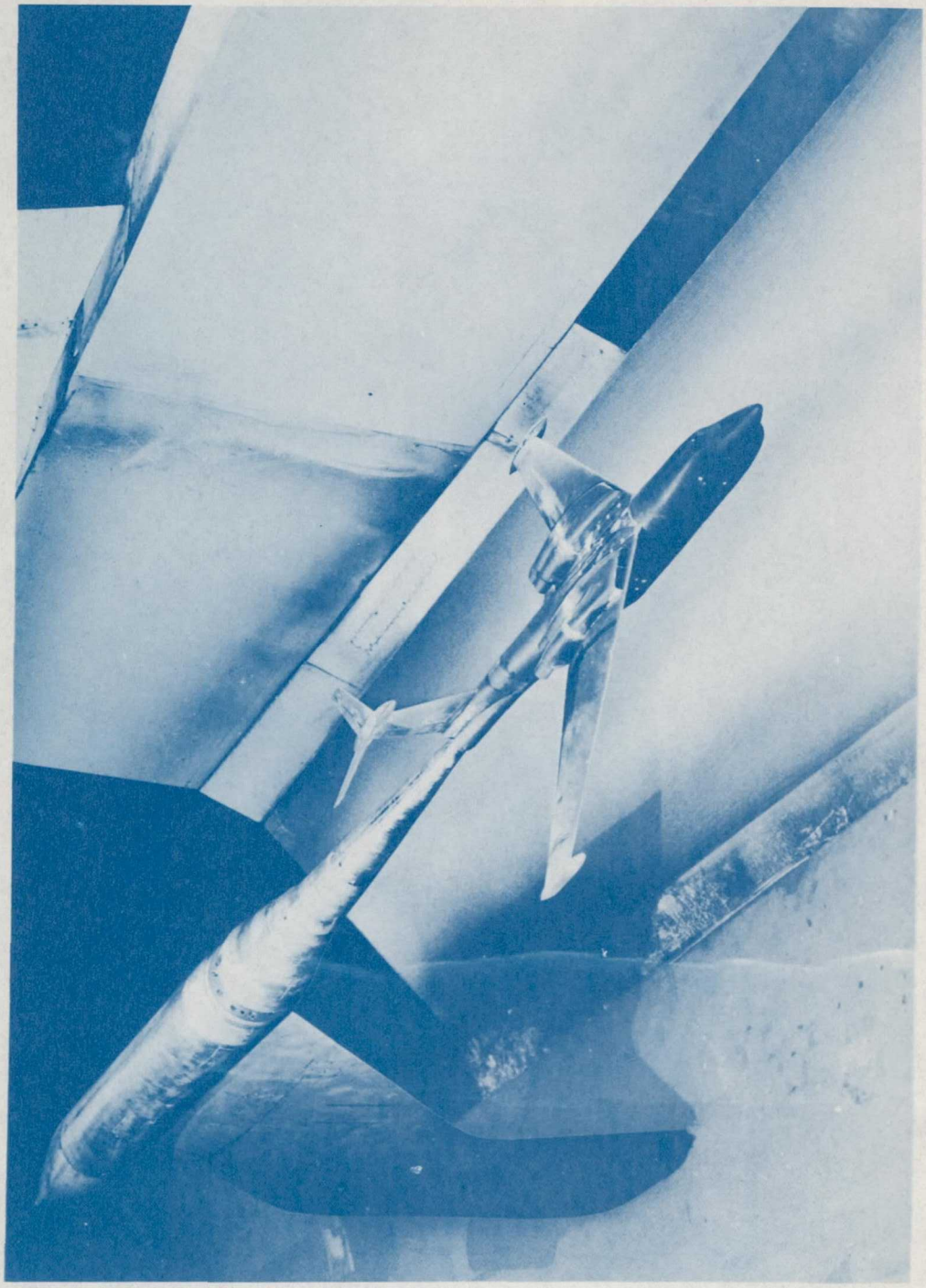

L-83542.1

Figure 2.- Three-quarter front view of model installed in the Langley 16-foot transonic tunnel.

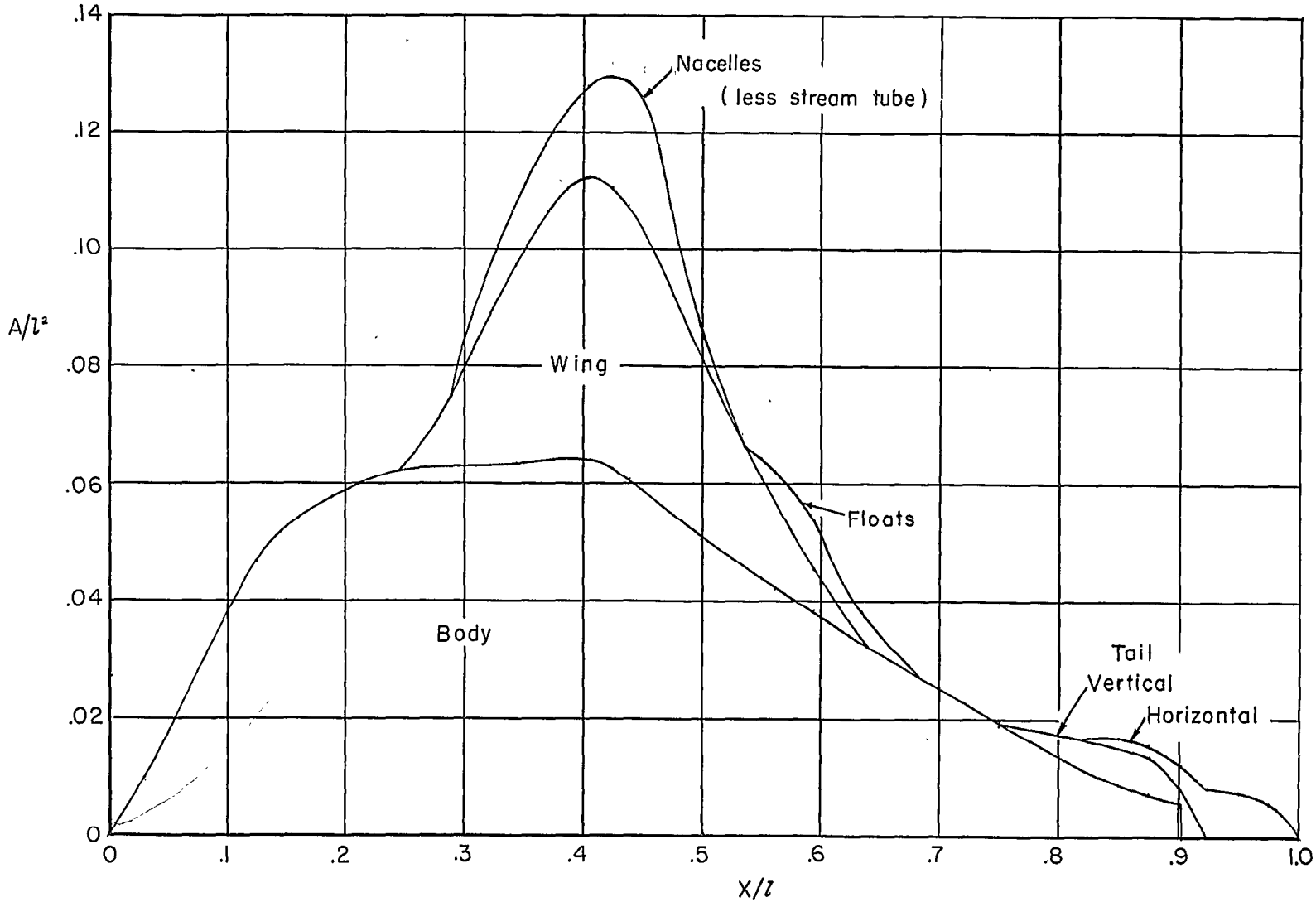

Figure 3.- Longitudinal distribution of cross-sectional area of seaplane.

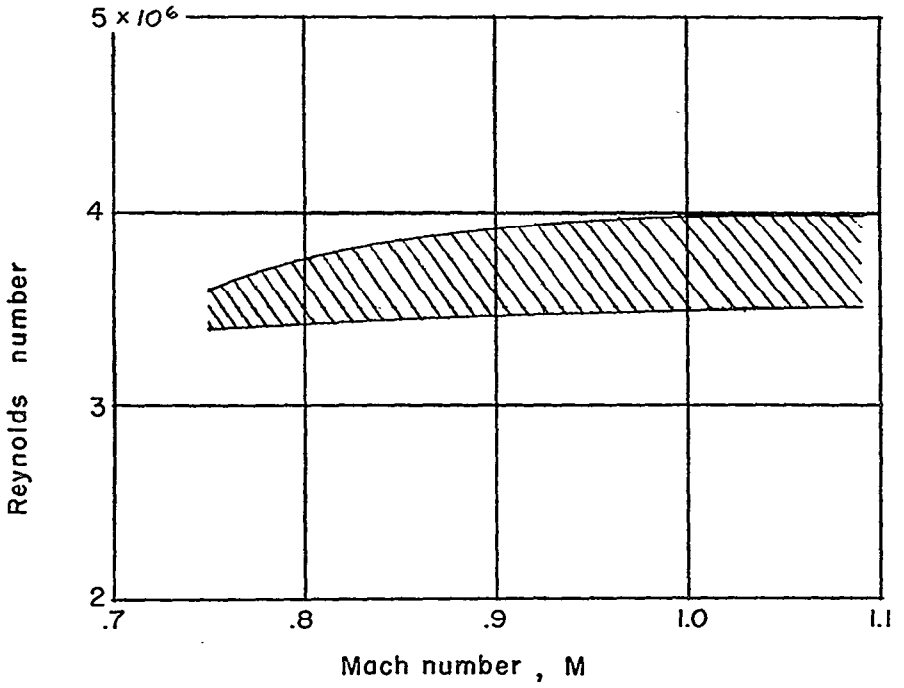

Figure 4.- Variation of Reynolds number with Mach number based on mean aerodynamic chord (0.927 foot).

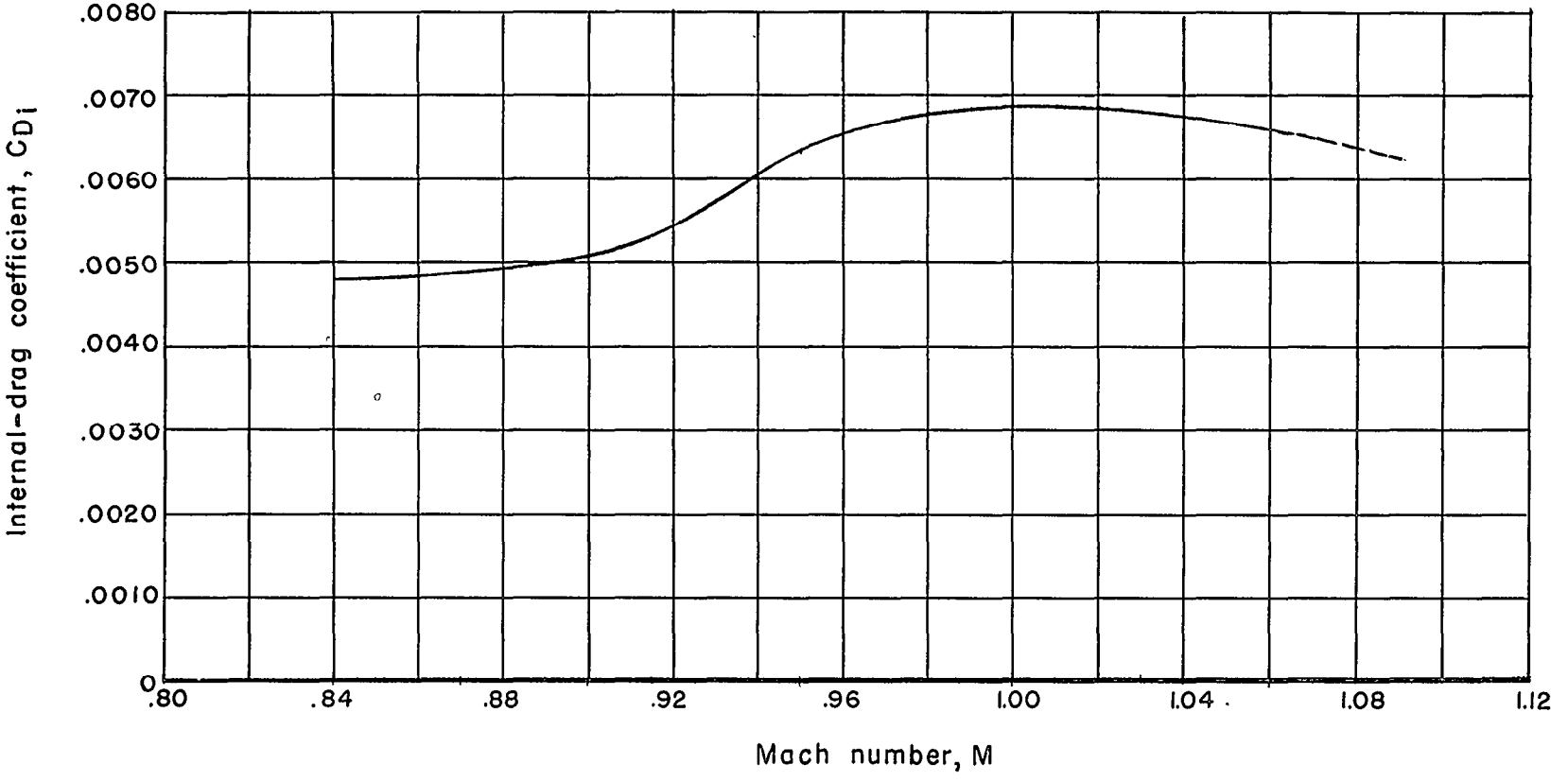

Figure 5.- Total internal-drag coefficient of the four nacelles.

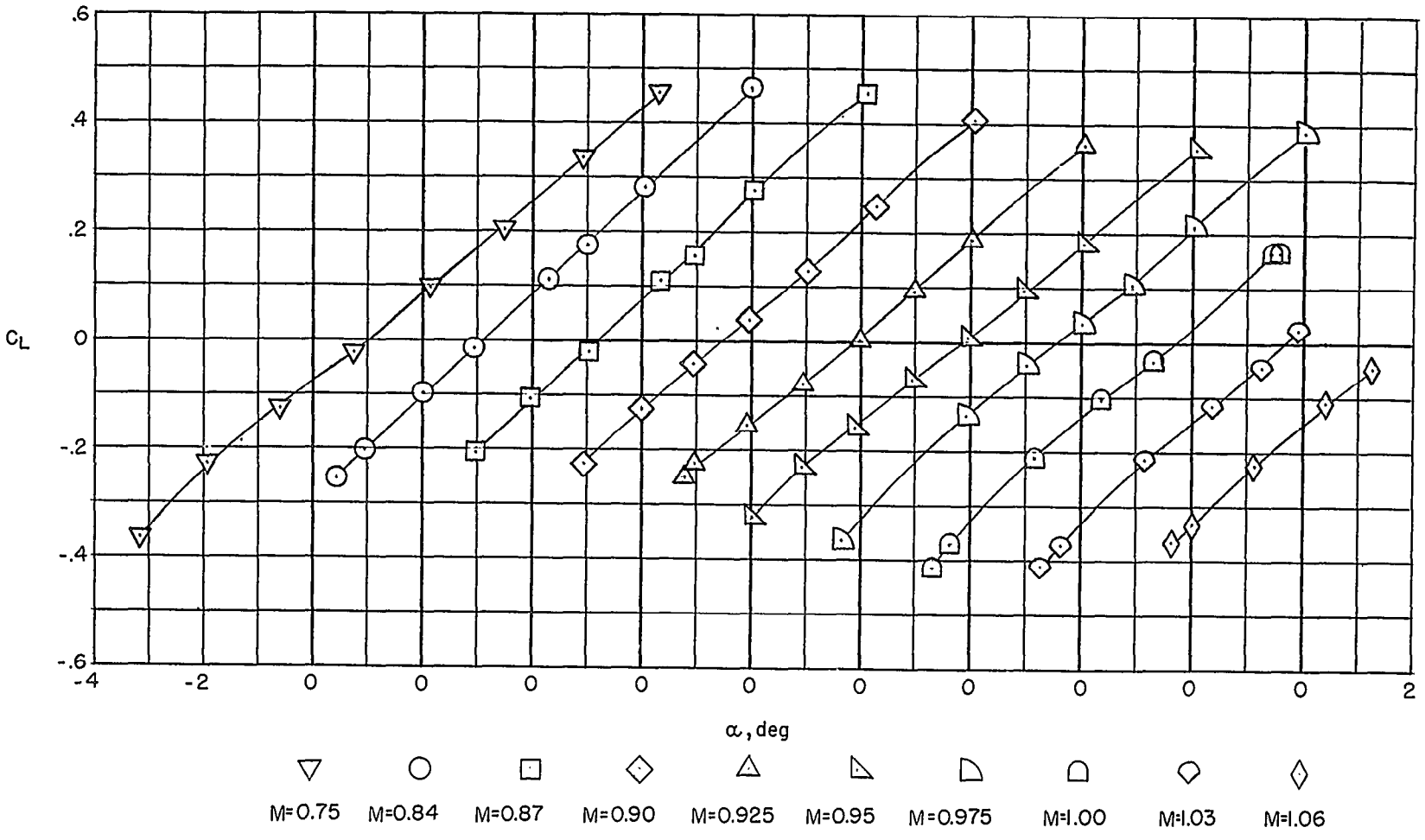

(a) Lift coefficient.

Figure 6.- Aerodynamic characteristics of model without horizontal tail.

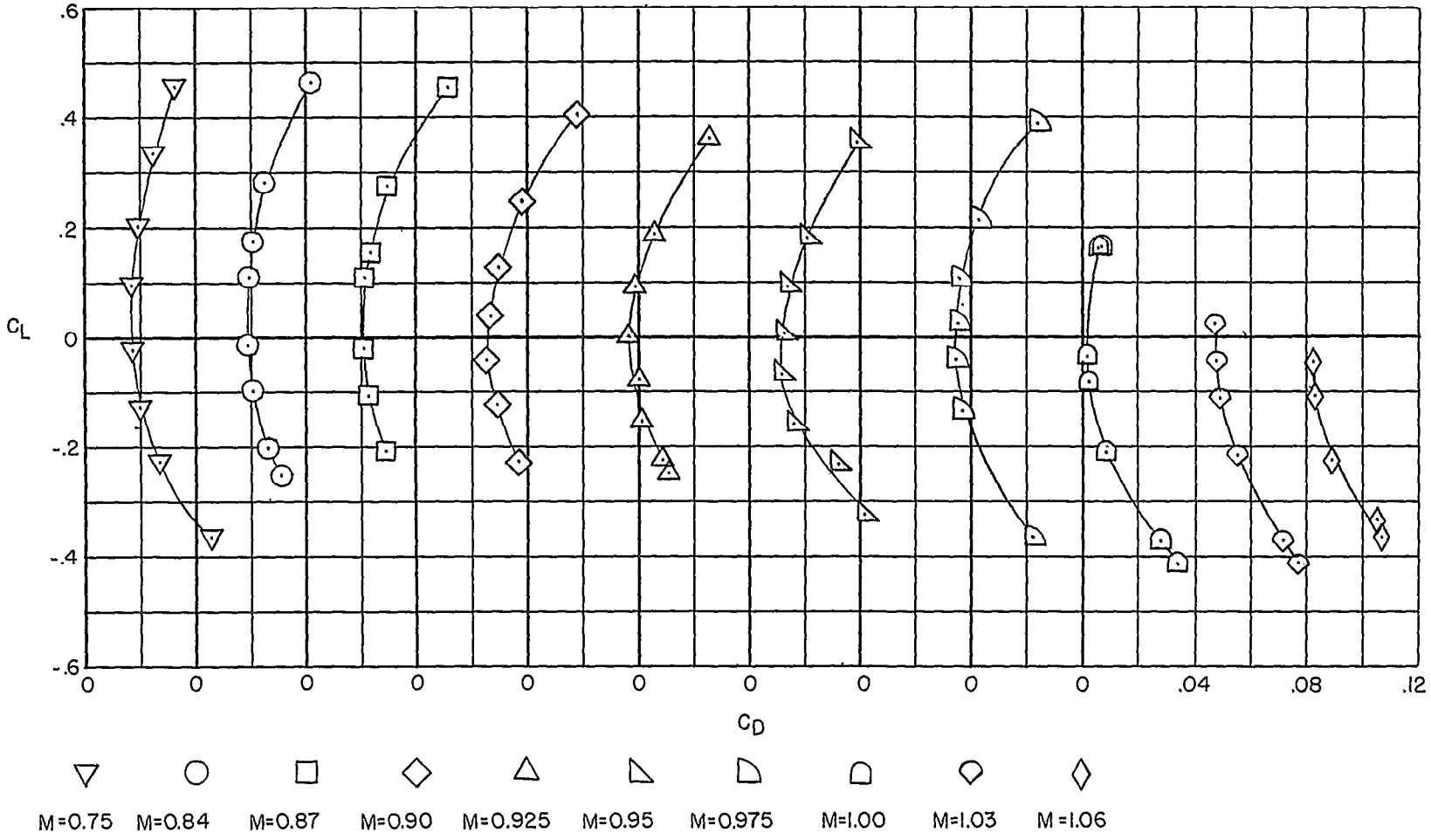

(b) Drag coefficient.

Figure 6.- Continued.

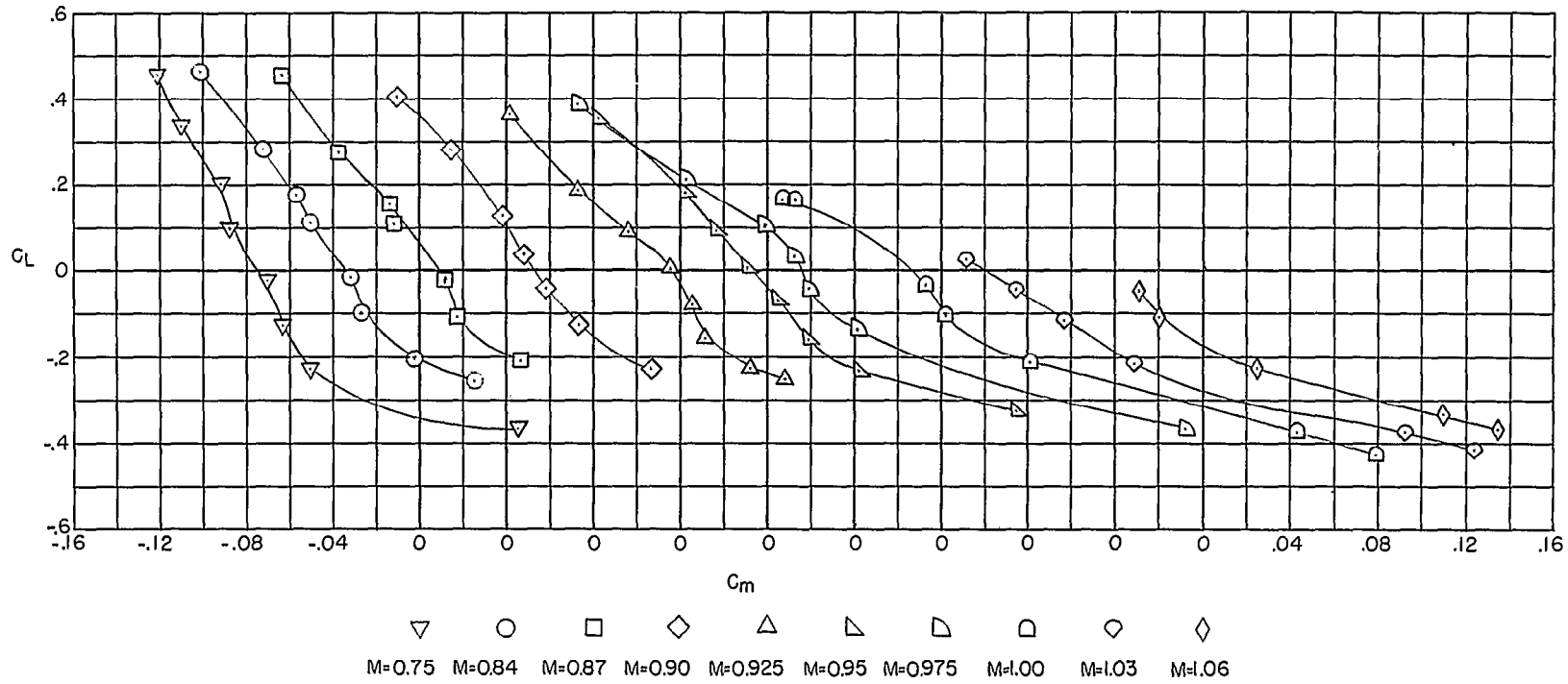

(c) Pitching-moment coefficient.

Figure 6.- Concluded.

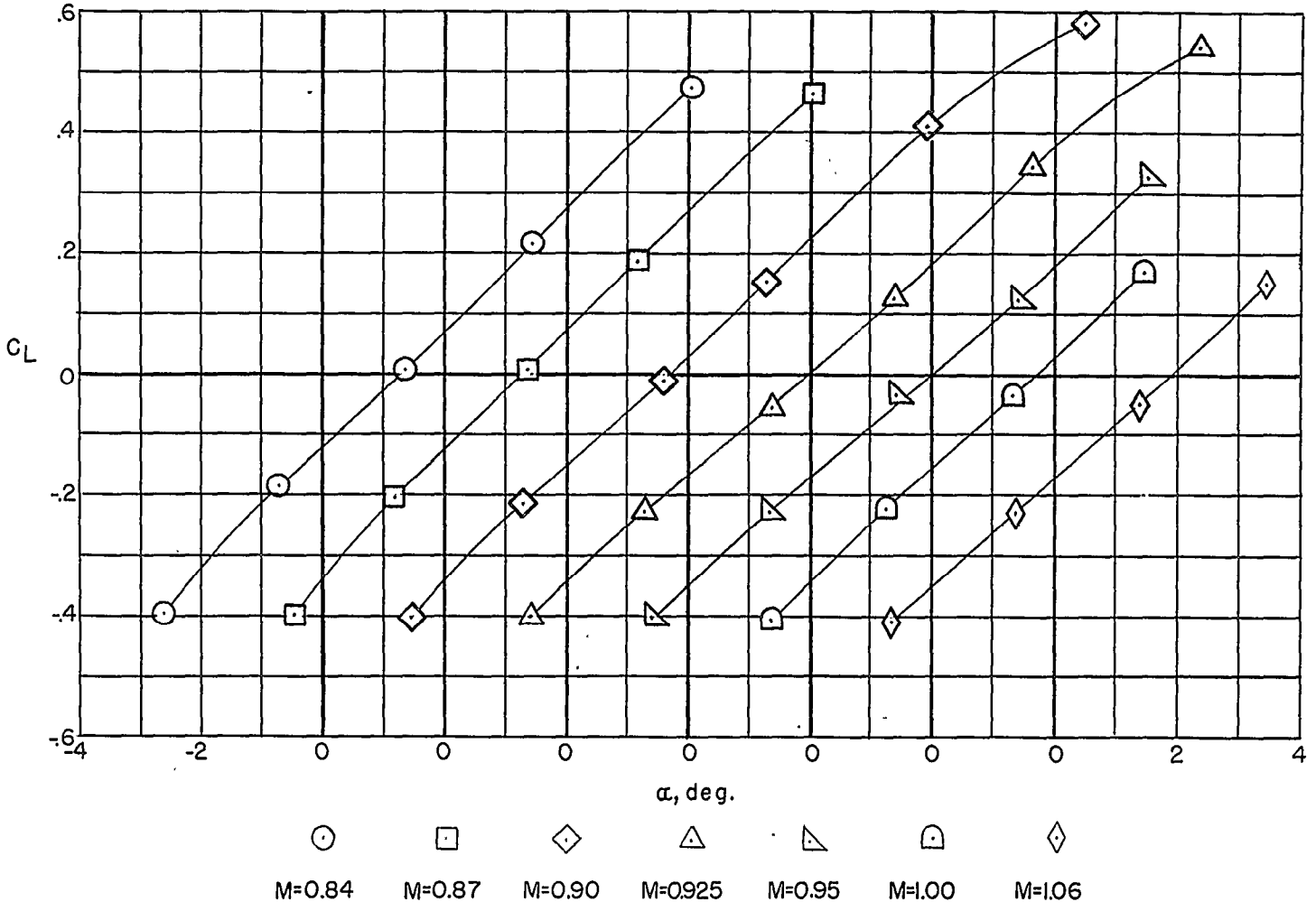

(a) Lift coefficient.

Figure 7.- Aerodynamic characteristics of complete model. $i_t = -0.82°$.

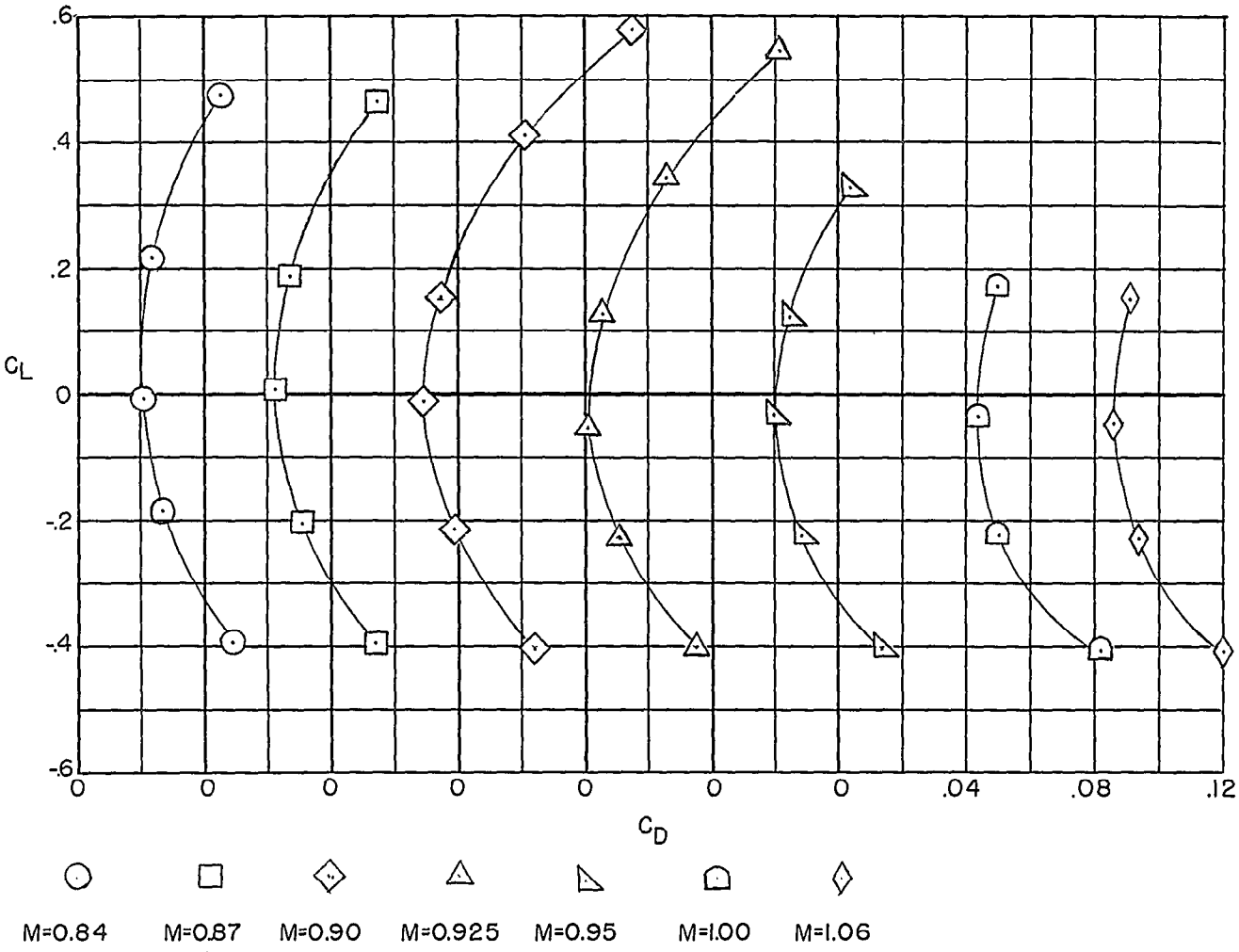

(b) Drag coefficient.

Figure 7.- Continued.

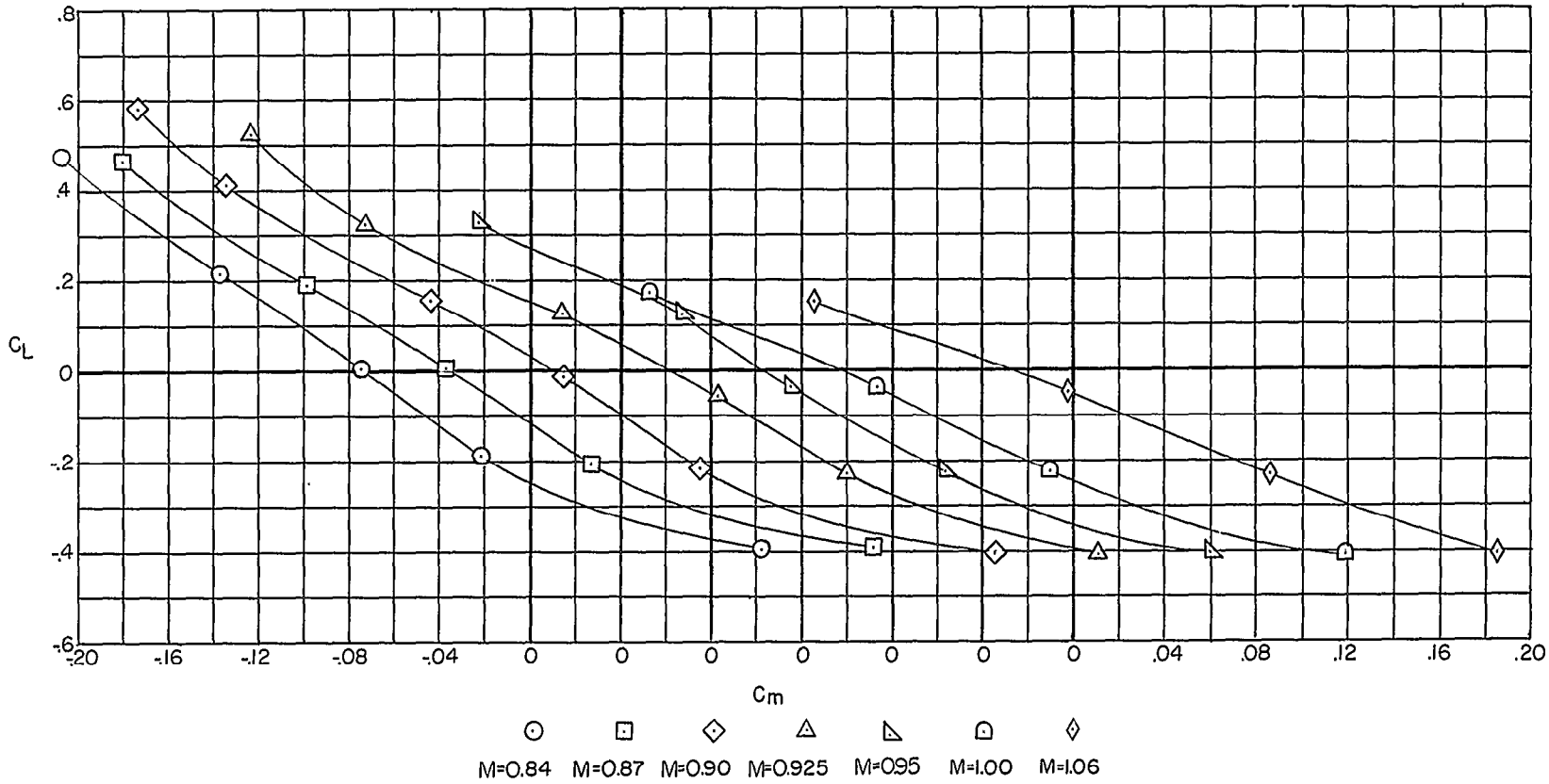

(c) Pitching-moment coefficient.

Figure 7.- Concluded.

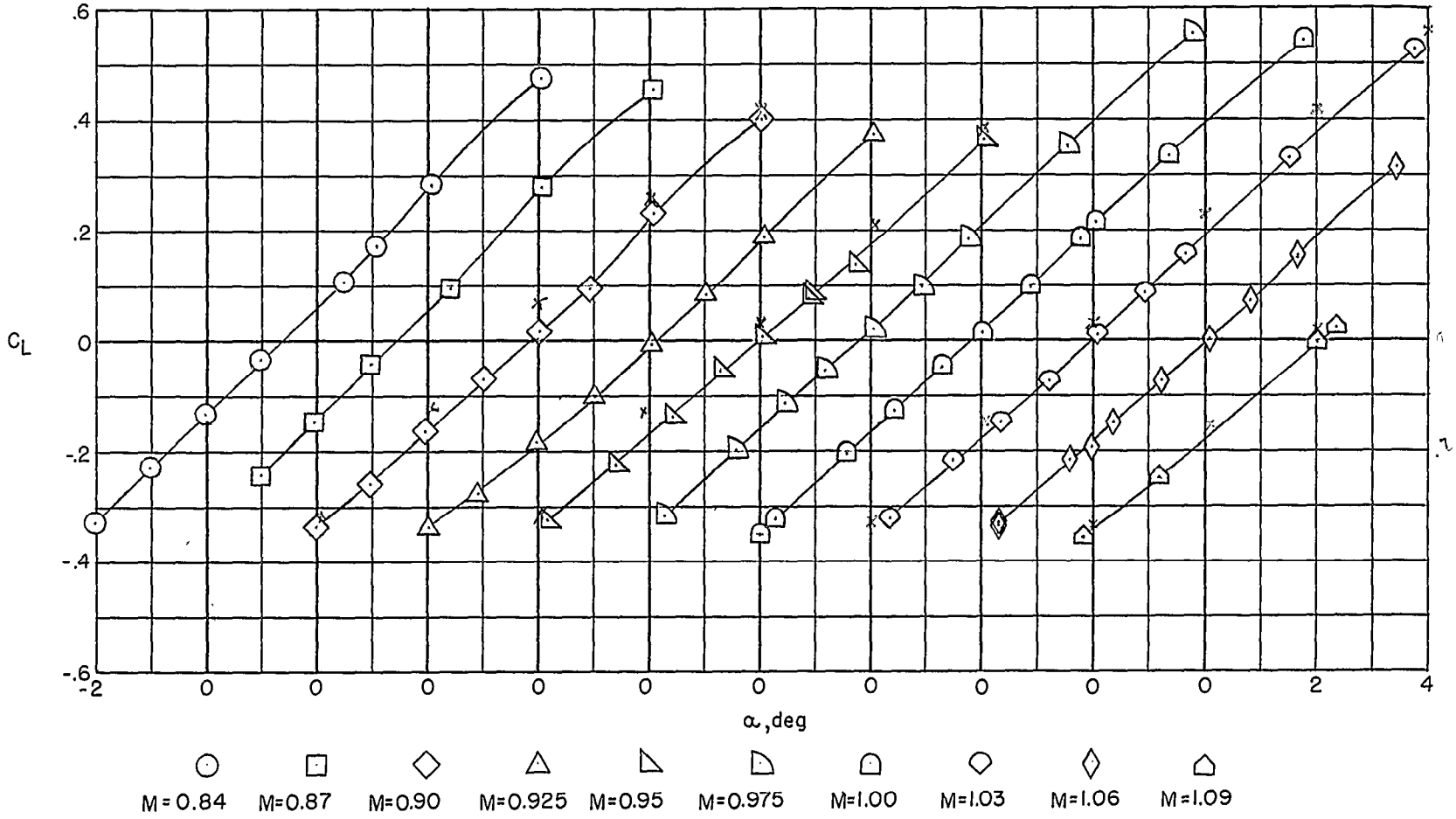

(a) Lift coefficient.

Figure 8.- Aerodynamic characteristics of complete model. $i_t = -3.02^\circ$.

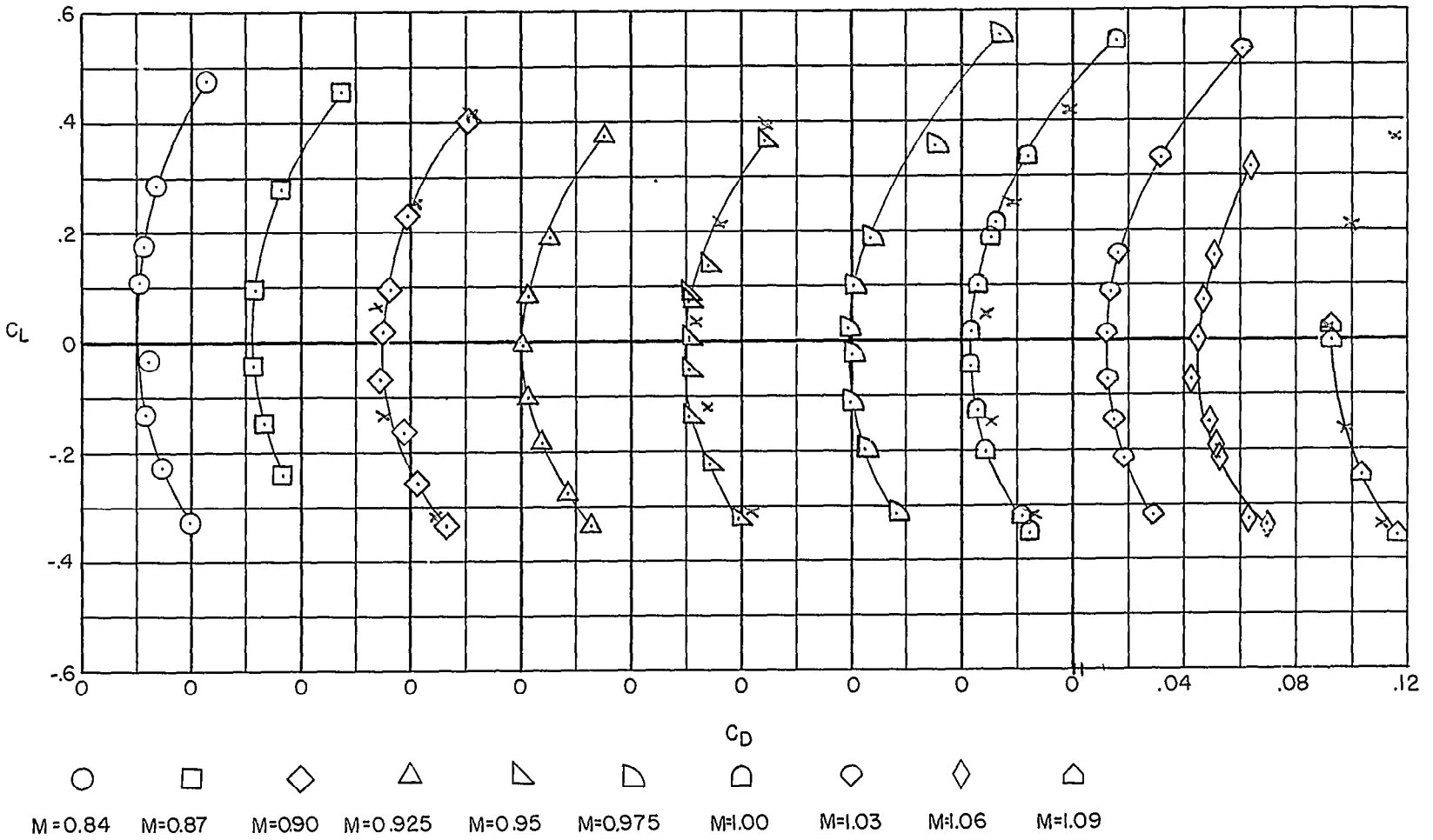

(b) Drag coefficient.

Figure 8.- Continued.

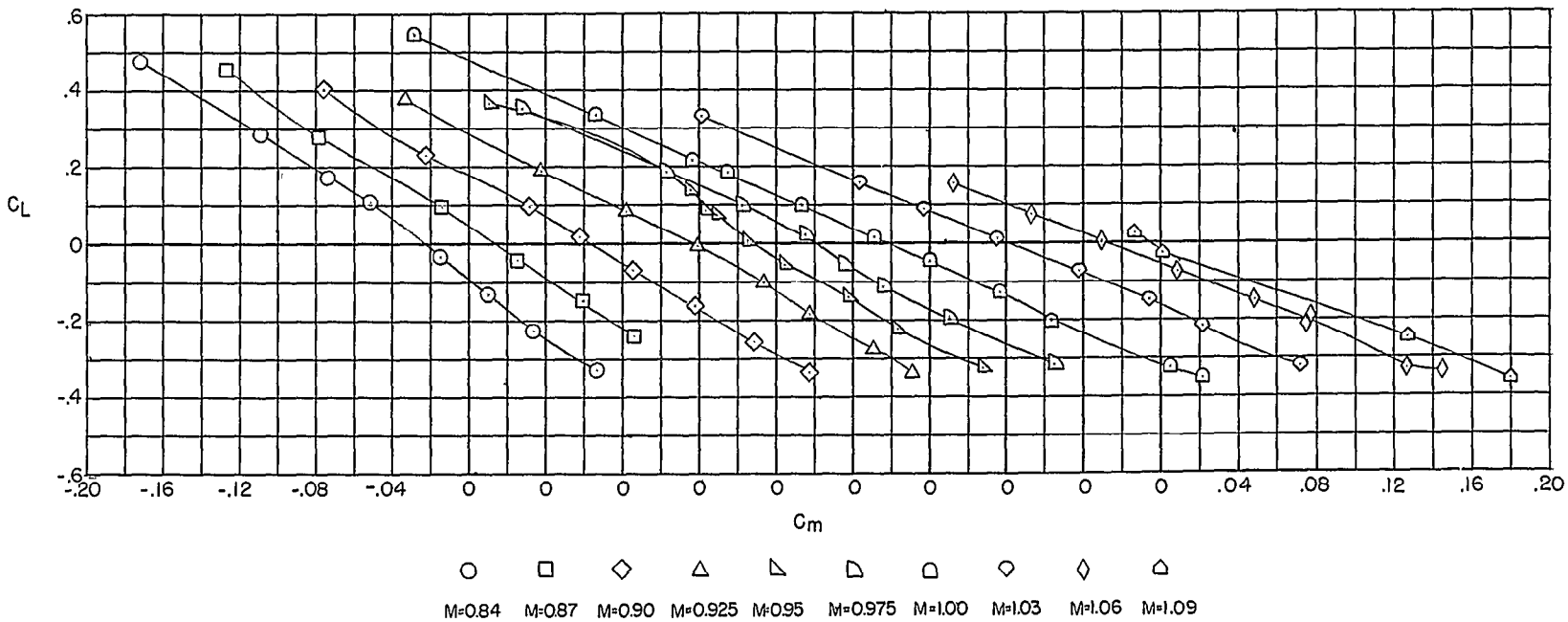

(c) Pitching-moment coefficient.

Figure 8.- Concluded.

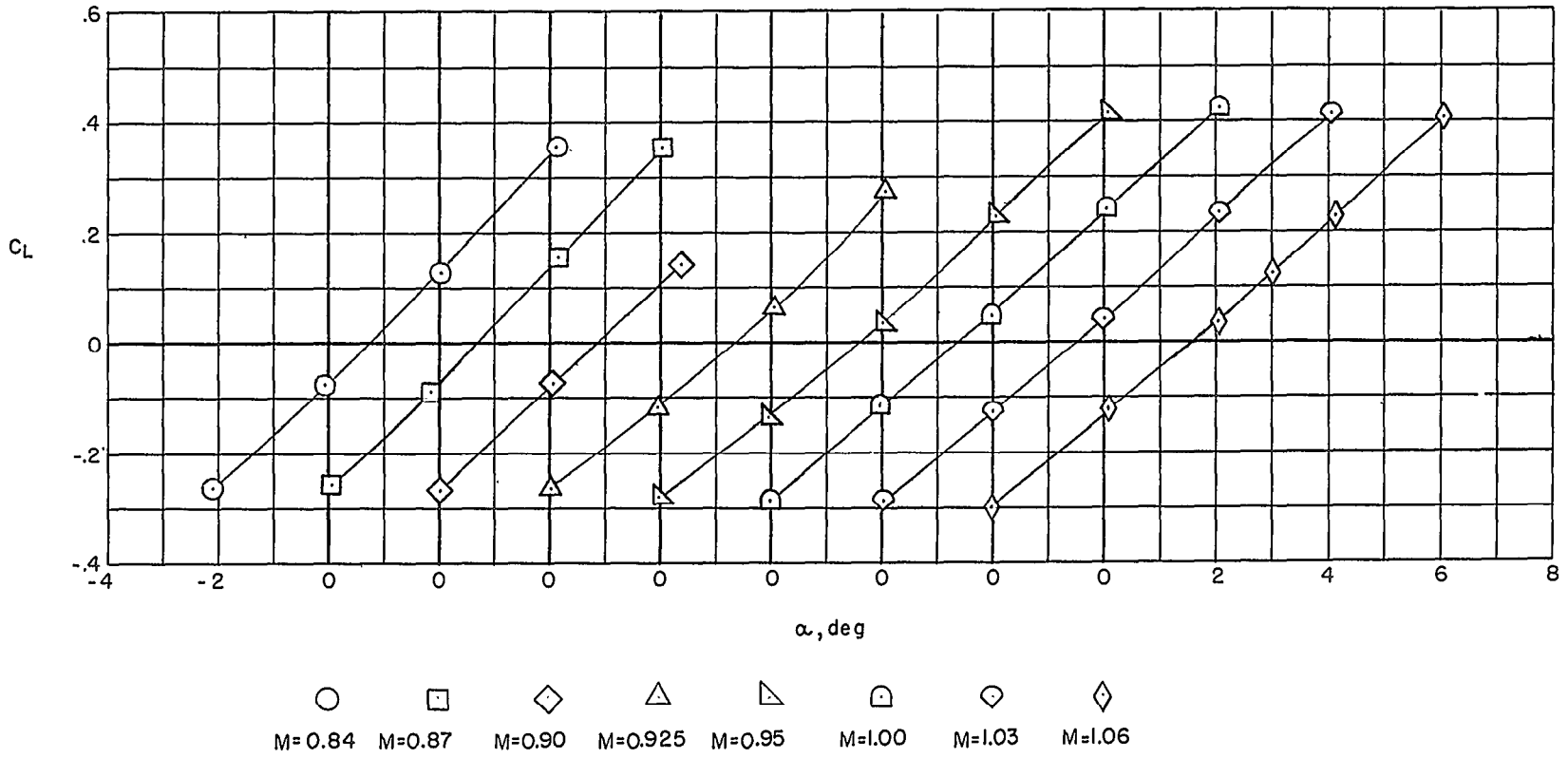

(a) Lift coefficient.

Figure 9.- Aerodynamic characteristics of model without engine nacelles. $i_t = -3.02^\circ$.

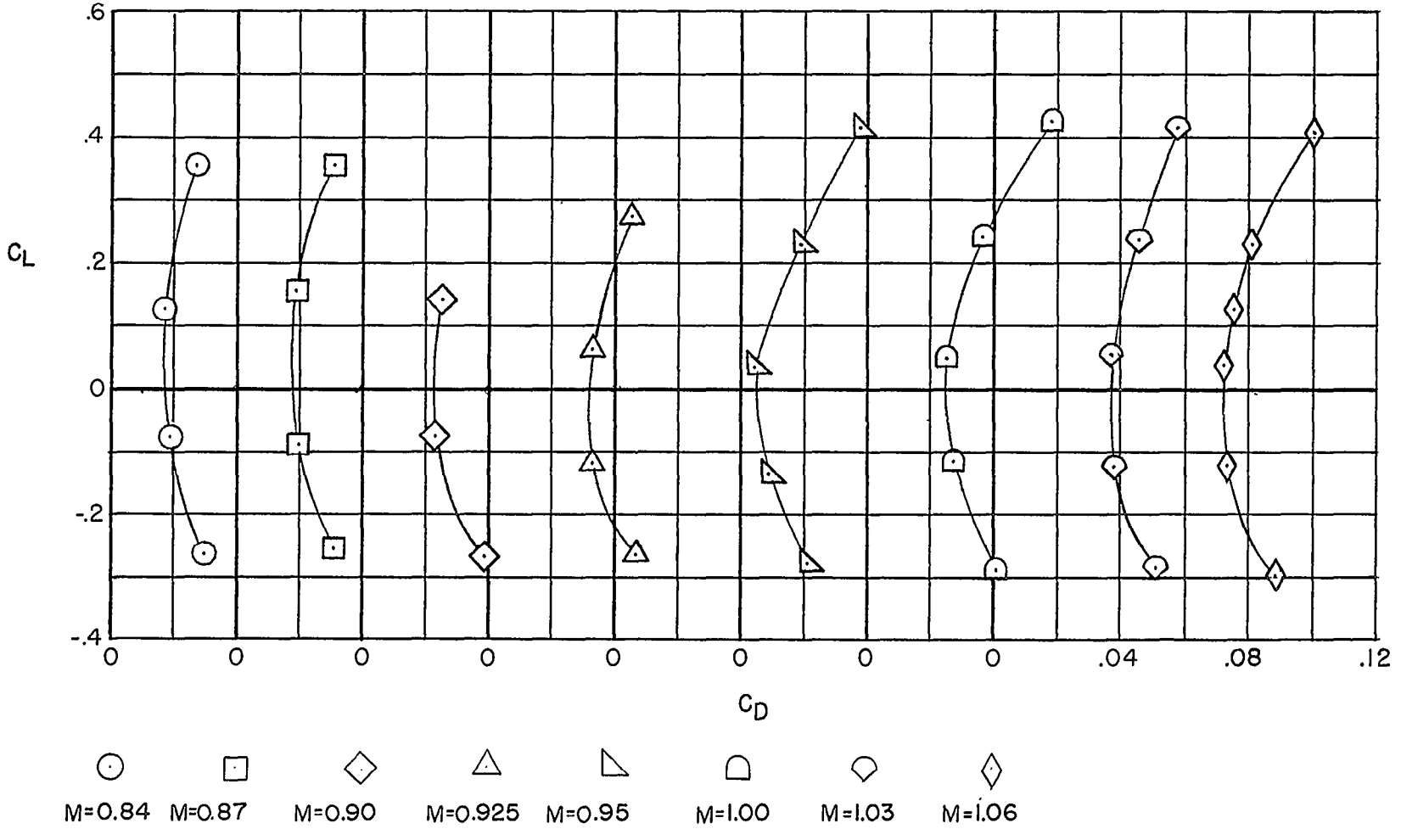

(b) Drag coefficient.

Figure 9.- Continued.

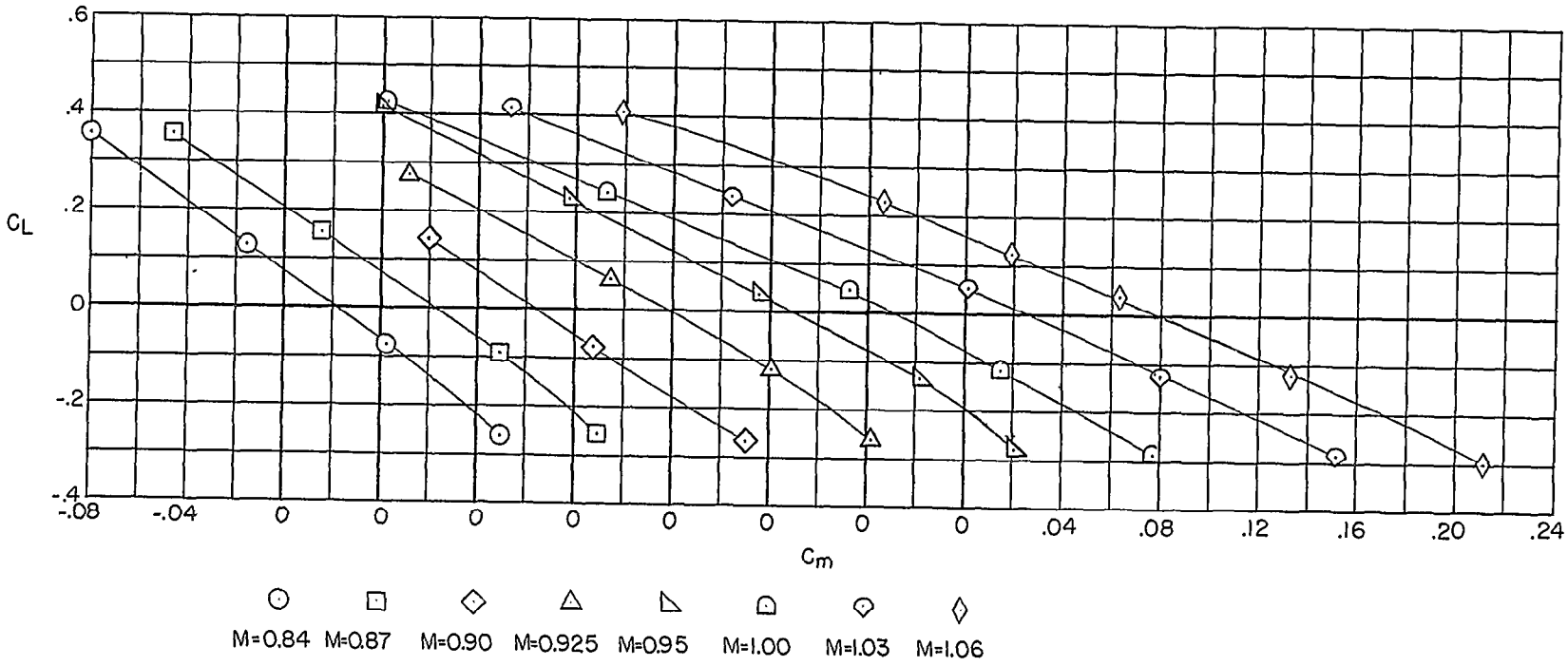

(c) Pitching-moment coefficient.

Figure 9.- Concluded.

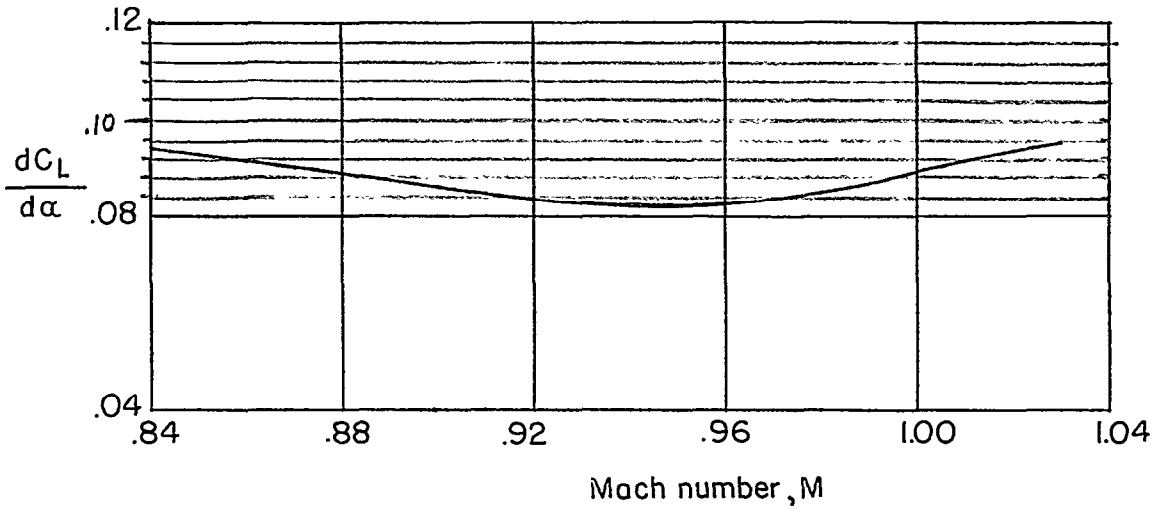

Figure 10.- Effect of Mach number on lift-curve slope. Model without horizontal tail.

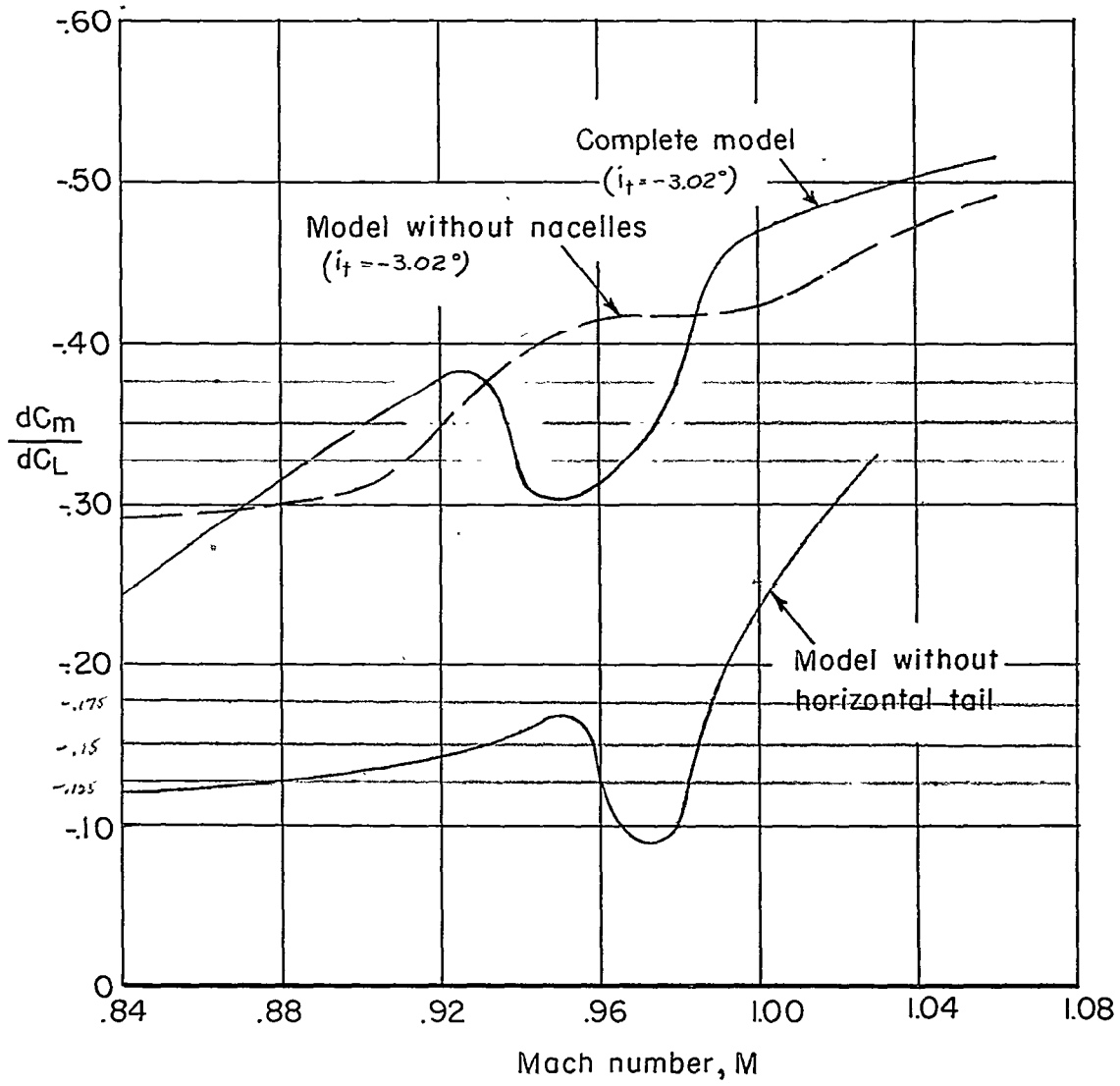

Figure 11.- Effect of Mach number on longitudinal-stability parameter.

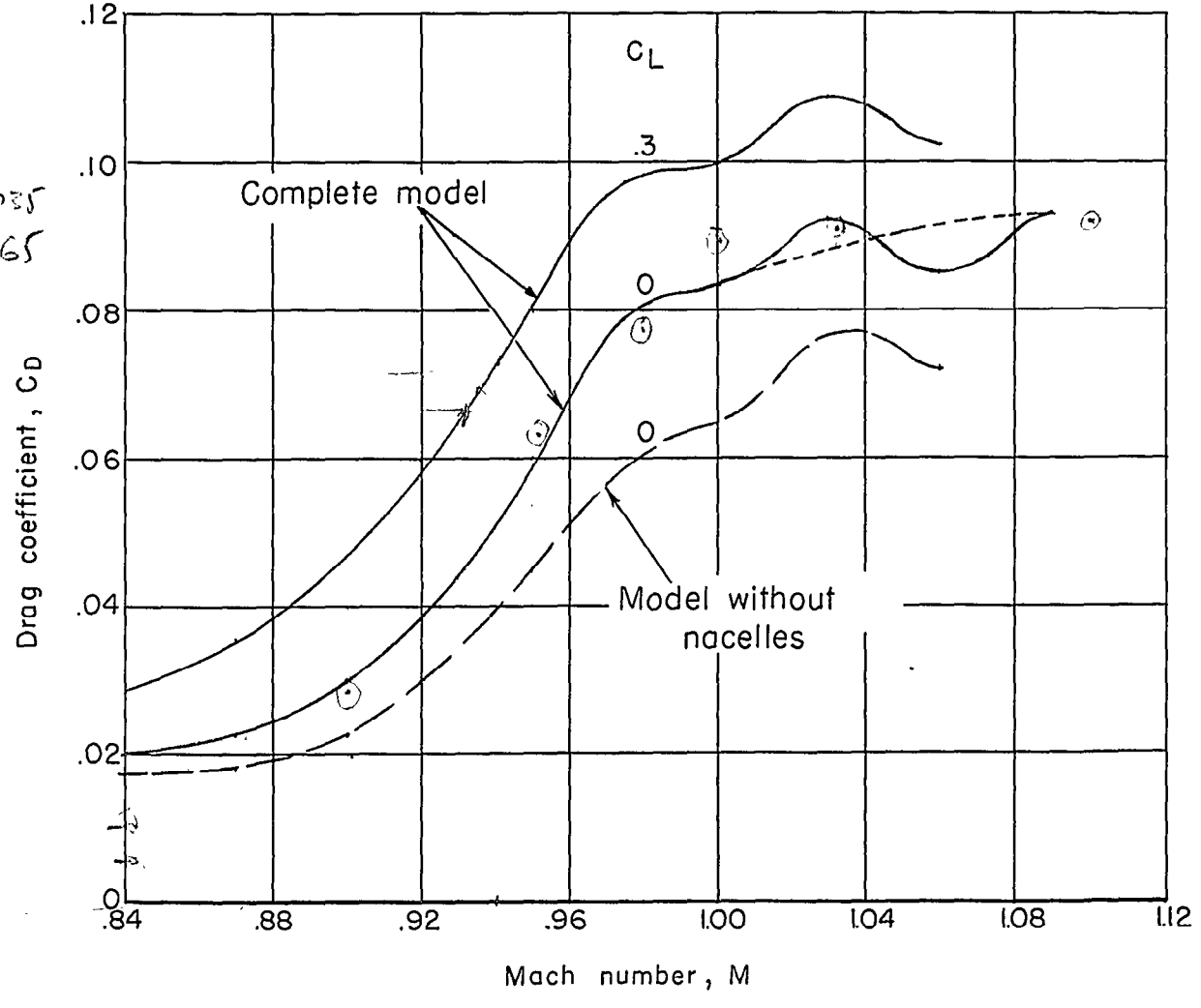

Figure 12.- Variation of drag coefficient with Mach number. Dotted curve indicates probable interference-free drag. $i_t = -3.02°$.

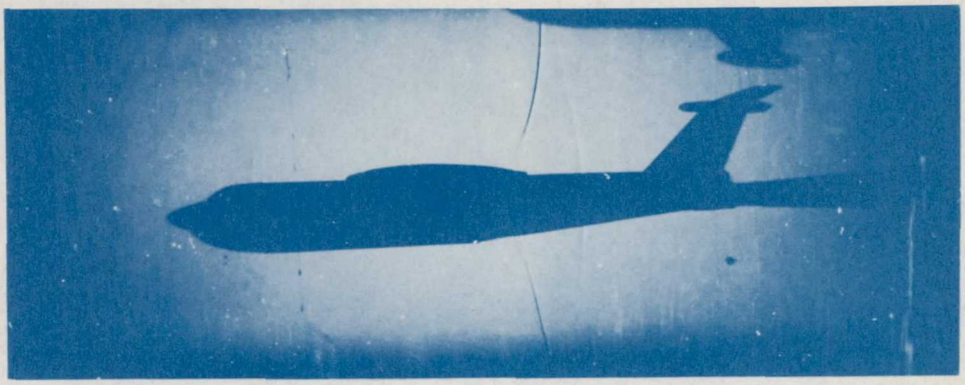

M = 0.95

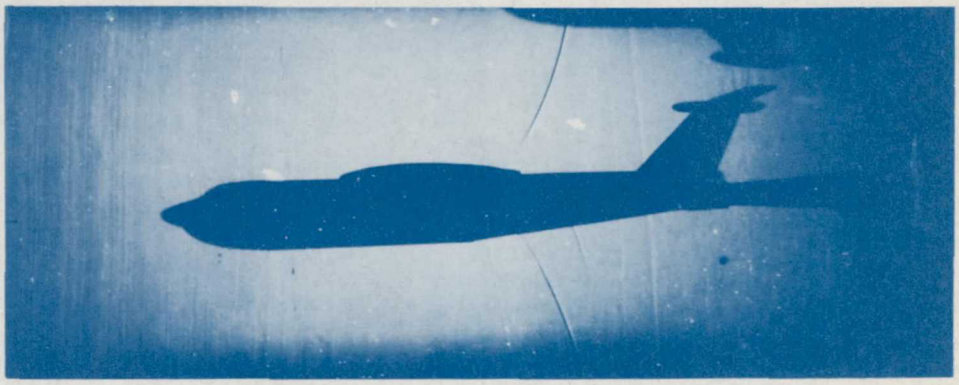

M = 0.975

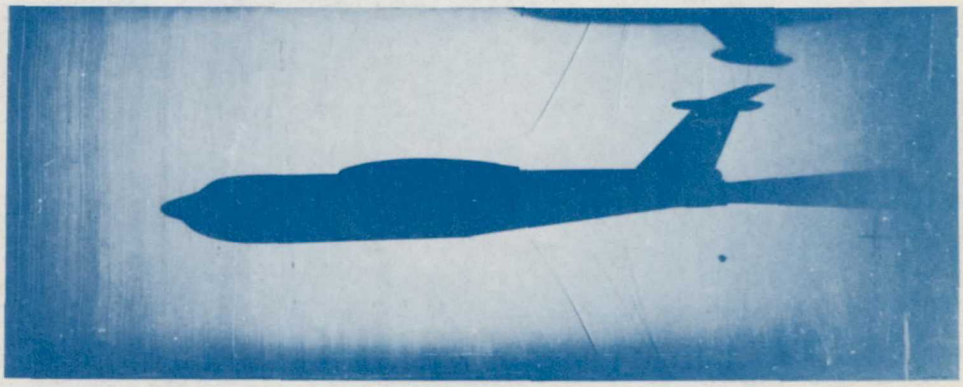

M = 1.00

L-87922

Figure 13.- Shadowgraphs of complete model obtained in transonic flow.